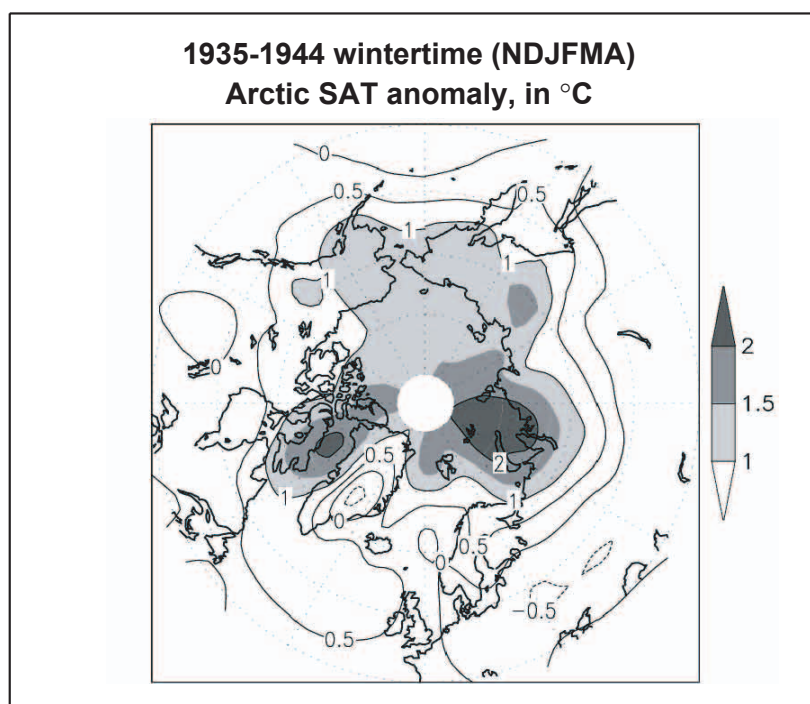




Report No. 345



The early century warming in the Arctic – A possible mechanism

by

Lennart Bengtsson • Vladimir A. Semenov • Ola Johannessen

Hamburg, February 2003

Authors

Lennart Bengtsson

Max-Planck-Institut für Meteorologie
Hamburg, Germany
&
Environmental Systems Science Centre
Harry Pitt Building, Whiteknights
Reading, UK

Vladimir A. Semenov

Max-Planck-Institut für Meteorologie
Hamburg, Germany
&
A.M. Obukhov Institute of Atmospheric Physics
RAS
Moscow, Russia

Ola Johannessen

Nansen Environmental and Remote Sensing
Center/Geophysical Institute
University of Bergen
Bergen, Norway

Max-Planck-Institut für Meteorologie
Bundesstrasse 55
D - 20146 Hamburg
Germany

Tel.: +49-(0)40-4 11 73-0
Fax: +49-(0)40-4 11 73-298
e-mail: <name>@dkrz.de
Web: www.mpimet.mpg.de

The early century warming in the Arctic – A possible mechanism

Lennart Bengtsson^{1,2}, Vladimir A. Semenov^{1,3} and Ola Johannessen⁴

¹ Max Planck Institute for Meteorology, Hamburg, Germany

² Environmental System Science Center, Reading, UK

³ Obukhov Institute of Atmospheric Physics, Moscow, Russia

⁴ Nansen Environmental and Remote Sensing Center/Geophysical Institute, University of
Bergen, Bergen, Norway

e-mail: bengtsson@dkrz.de

Tel.: +49 40 41173-349

Fax: +49 40 411 73 366

MPI Report 345

February 2003

(will be submitted to *Journal of Climate*)

ISSN 0937-1060

Abstract

The huge warming of the Arctic that started in the early 1920s and lasted for almost two decades is one of the most spectacular climate events of the 20th century. During the peak period 1930-1940 the annually averaged temperature anomaly for the area 60°N-90°N amounted to some 1.7°C. Whether this event is an example of an internal climate mode or externally forced, such as by enhanced solar effects, is presently under debate. Here we suggest that natural variability is the most likely cause with reduced sea ice cover being crucial for the warming. A robust sea ice-air temperature relationship was demonstrated by a set of four simulations with the atmospheric ECHAM model forced with observed SST and sea ice concentrations. An analysis of the spatial characteristics of the observed early century surface air temperature anomaly revealed that it was associated with similar sea ice variations. We have further investigated the variability of Arctic surface temperature and sea ice cover by analyzing data from a coupled ocean-atmosphere model. By analyzing similar climate anomalies in the model as occurred in the early 20th century, it was found that the simulated temperature increase in the Arctic was caused by enhanced wind driven oceanic inflow into the Barents Sea with an associated sea ice retreat. The magnitude of the inflow is linked to the strength of westerlies into the Barents Sea. We propose a positive feedback sustaining the enhanced westerly winds by a cyclonic atmospheric circulation in the Barents Sea region created by a strong surface heat flux over the ice-free areas. Observational data suggest a similar series of events during the early 20th century Arctic warming including increasing westerly winds between Spitsbergen and the northernmost Norwegian coast, reduced sea ice and enhanced cyclonic circulation over the Barents Sea. It is interesting to note that the increasing high latitude westerly flow at this time was unrelated to the North Atlantic Oscillation, which at the same time was weakening.

1. Introduction

The warming event in the first part of the 20th century, considered at the time by some as the first sign of climate warming caused by increasing CO₂ (Callender, 1938), was mainly confined to the higher latitudes of the Northern Hemisphere. The largest warming occurred in the Arctic (60°N-90°N) (Johannessen et al., 2003) averaged for the 1940s with some 1.7°C (2.2°C for the winter half of the year) relative to the 1910s. As can be seen from the Fig. 1, it was a long lasting event commencing in the early 1920s and reaching its maximum some 20 years later. The decades after were much colder, although not as cold as in the early years of the last century. It is interesting to note that the ongoing present warming has just reached the peak value of the 1940s, and this has underpinned some views that even the present Arctic warming is dominated by other factors than increasing greenhouse gases (Polyakov and Johnson, 2000, Polyakov et al., 2002). However, other authors (e.g. Johannessen et al., 2003) concluded that the present warming in the Arctic is dominated by anthropogenic GHG forcing.

Four possible mechanisms, individually or in combination, contributed to the early 20th century warming: anthropogenic effects, increased solar irradiation, reduced volcanic activity and internal variability of the climate system.

It seems unlikely that anthropogenic forcing on its own could have caused the warming, since the change in greenhouse gas forcing in the early decades of the 20th century was only some 20% of the present (Roeckner et al., 1999). Secondly, it remains to explain the marked cooling trend between 1940-1960, a period with a similar or faster increase of the greenhouse gases than between 1920-1940 (Joos and Bruno, 1998). The direct and indirect effect of sulphate aerosols though had a rapidly increasing trend (Roeckner et al., 1999), which partly compensated the increase of greenhouse forcing during the 1940-1960 period. Nevertheless, the total anthropogenic forcing was larger in the 1940-1960 period, when cooling occurred, than in the 1920-1940 warming period, thereby rejecting the idea that anthropogenic forcing caused the 1920-1940 warming.

Changes in solar forcing have been suggested (e.g., Lean and Rind, 1998, Beer et al., 2000 and references therein) as the cause of the warming. It has attracted considerable interests

because of the apparent similarity between the assumed solar variability and the temperature trend of the Northern Hemisphere extra-tropics (Reid, 1991, Friis-Christensen and Lassen, 1991, Hoyt and Schatten, 1993). Available data sets of solar variability (Hoyt and Schatten, 1993, Lean et al., 1995) have been used in modelling studies (Cubasch et al., 1997, Cubasch and Voss, 2000, Stott et al., 2001, Tett et al., 1999) providing results broadly consistent with long term estimated or observed temperature trends. This is not surprising since multi-decadal and longer trends in solar forcing generate a response in global average modelled temperatures on similar time-scales as the variation in solar forcing (Cubasch et al., 1997).

However, the main weakness with solar forcing hypothesis is the lack of reliable observational data of solar irradiation. These only exist for the last two decades (Fröhlich and Lean, 1998), which is insufficient to show any longer term trends. Therefore solar forcing can at the present time only be considered as a hypothesis of climate change and will presumably need another couple of decades of accurate irradiation measurements before it can be accepted or dismissed.

From 1912 onwards, volcanic activity entered a more quiescent phase and thus eliminated this climate cooling factor. Following the major eruptions at the beginning of the last century (Santa Maria in 1902, Ksudach in 1907 and Katmai in 1912) no substantial volcanic eruption occurred until Mount Agung in 1963 (Robock, 2000). Of these eruptions Katmai was the most intense at least with respect to the anticipated effect on climate (stratospheric aerosols). Nevertheless, the eruption by Mount Pinatubo in 1991 was more powerful by about a factor of two compared to Katmai (Robock, 2000). We may therefore assume that the climate effect from Katmai was less than that from Pinatubo and we have no reason to believe that the effect should have lasted longer than the effect of Pinatubo. According to several modelling studies as well as to observational assessments the cooling effect of Pinatubo had disappeared after a period shorter than three years (Bengtsson et al., 1999). Consequently the cooling effect of Katmai could hardly have lasted longer than 1915.

Internal variations in the climate system can affect the global climate significantly. The global average temperature in 1998, for example, was 0.3°C warmer than the preceding and the following year (Hansen et al., 1999), most likely as a consequence of the 1997/98 El Nino event. Coupled model experiments have demonstrated marked natural fluctuations on decadal

time-scales (Johannessen et al., 2003). There are strong indications that such fluctuations also exist in nature (Schlesinger and Ramankutty, 1994, Andronova and Schlesinger, 2000, Delworth and Mann, 2000), although the mechanisms causing them are open to debate (e.g. Mysak and Venegas, 1998, Mysak, 2001, Delworth and Mann, 2000, Johnson et al., 1999). However, there are strong indications that they are chaotic and unpredictable, at least on a time-scale longer than the fluctuation itself. The lack of long-term predictability is also indicated by the results of ensemble integrations with a coupled atmosphere-ocean model (Delworth and Knutsson, 2000).

To attribute a particular forcing mechanism with an observed pattern of climate change is hardly feasible, since the pattern of forcing and the pattern of response are essentially uncorrelated (Hansen et al., 1997, Bengtsson, 2001). The forcing by CO₂, for example, is largest in the tropics but the largest surface warming occurs at higher latitudes. The same is true for solar forcing. Characteristic for all the models used in a CMIP intercomparison study (Räisänen, 2002) was a maximum warming in the Arctic, a modest warming in the tropics and a minimum warming at the higher latitudes of the Southern hemisphere. In fact, in the study reported by Bengtsson (2001, fig 7) the actual forcing was negative over parts of the Northern Hemisphere (greenhouse gases and sulphate aerosols 1950-1990) but the actual warming was among the largest in these areas. Similarly, the forcing was positive for the Southern Hemisphere (practically only greenhouse gases), yet here the warming was the smallest. The approach generally applied to study natural and anthropogenic variability is one of pattern recognition between forced coupled models and control experiments without forcing (Hasselmann, 1997, Hegerl et al., 1997). This is probably a possible approach in cases of more substantial forcing, and when global patterns are considered. However, it requires that the climate models are capable of reproducing characteristic internal patterns of the climate system. If models underestimate such fluctuations, observed patterns outside the range of such models could then incorrectly be subscribed to external forcing. Alternatively, if models overestimate internal low-frequency fluctuations the opposite will hold. It seems that for present models neither of these alternatives can be excluded.

In the case of regional anomalies an additional level of complexity arises. Here the role of atmospheric and ocean circulation anomalies must be considered. As demonstrated by Hurrell (1995), for example, the positive surface temperature anomaly of the Northern Hemisphere

extra-tropics 1981-1995 strongly depended on the mode of circulation of the North Atlantic Oscillation (NAO) and Southern Oscillation (SO). The NAO in particular has a marked stochastic variability, although there are indications from numerical experiments that SST anomalies, mainly in the tropical oceans, may influence the probability distribution function of the NAO (Hoerling et al., 2001; Schneider et al., 2003).

However, the atmospheric response to forcing from ocean SST anomalies is not particularly robust, as has recently been demonstrated by Schneider et al., 2003. The North Atlantic-European-Arctic region is strongly exposed to stirring by transient synoptic atmospheric eddies, and has a less robust response to forcing from SST anomalies than for example the North Pacific-North American region (Schneider et al., 2003). The large chaotic atmospheric variability in the North Europe-Arctic region is also indicated by the CMIP intercomparison (Räisänen, 2002), and by the large differences between the five members of the ensemble simulation study reported by Delworth and Knutson (2000). The differences are particularly large in the Arctic region where they extend over several decades. It is thus strongly suggested that climate variations in the Arctic are dominated by larger scale dynamical processes in the atmosphere and the ocean and not only by local radiative processes and ice albedo feedback. A particular issue to be addressed in this paper is a possible climate feedback mechanism that can contribute towards long lasting climate anomalies in the Arctic.

Here we will provide in a semi-quantitative way using observations and model simulations a possible explanation of the high latitude warming in the 1930-1940. During the first and second decade of the last century there was a high proportion of years with stronger than normal westerly circulation over the North Atlantic (NAO in a positive phase, Hurrell, 1995). As has been shown by Curry and McCartney (2001), the long term domination of such a atmospheric flow pattern drives the ocean circulation and results in the advection of warm water into the North Atlantic. The fact that the NAO was in a positive phase for several years could very likely be a consequence of chance along the lines pointed out by Wunsch (1999), where it was shown that longer episodes of either positive or negative NAO anomalies could occur due to aggregation of random atmospheric events.

In spite of recent attempts to make the NAO the key driver for explaining Arctic climate variations (e.g. Moritz et al., 2002), the NAO cannot explain why the Arctic rapidly started to

warm up from the 1920 onward, since in fact the NAO at the same time had a *reverse* trend (and should instead have supported an Arctic cooling!) and remained close to the average climate state for several decades (without any longer periods of either high or low values, see also Fig. 8b). Instead, and much more indisputable, we propose here that the warming was caused by the steadily increasing transport of warm water into the Barents Sea driven by increasing south westerly to westerly winds between Spitsbergen and the northernmost Norwegian coast. Between 1920 and 1940 the observed pressure gradient increased by some 8 mb corresponding to an average geostrophic wind anomaly of 6 ms^{-1} . This led to increased transport of warm water into the Barents Sea, with a major reduction of sea ice in this region, where the largest atmospheric temperature anomalies also occur. As we will further demonstrate using model simulations, the reduced sea ice coverage is the main reason for the increased Arctic temperature. A close link between observed sea ice and temperature variability has also been established by century long sea ice analysis (Johannessen et al., 2003, Zakharov, 1997), supporting the model simulations.

We will describe the typical Arctic warming pattern in section 2, and in section 3 and 4 discuss analyses of numerical experiments with atmospheric and coupled ocean-atmosphere models, respectively. In section 5, we outline a positive feedback mechanism and in section 6, undertake a comprehensive discussion of the results and possible consequences for climate change in the Arctic.

2. Arctic warming pattern

Temperature observations in the Arctic and adjacent regions include a number of records from land-based weather stations, several of them extending back to 19th century (Przybylak, 2000, for review). Since the 1950s data for the interior Arctic have been collected primarily by manned drifting polar stations, buoys and drop sondes (Martin et al., 1997; Kahl et al., 1993; Rigor et al., 2000). Due to different temporal-spatial coverage and measurements techniques, the analyses of these data usually embrace only recent decades and sometimes lead to contradictory conclusions about magnitude and direction of the Arctic temperature trends (Serreze et al., 2000, Kahl et al., 1993, Polyakov et al., 2002).

Global gridded surface air temperatures, SAT (Jones et al., 1999, Hansen et al., 1999), which have been widely used for climate change and variability studies, have major gaps over the highest northern latitudes, in particular over the ice covered ocean areas. This complicates an adequate analysis of the SAT spatial-temporal variability in the Arctic during the 20th century, especially for the first half of the century.

Here, we use a century-long gridded Russian SAT dataset, which is more complete than the Jones data in the high latitudes (Alekseev et al., 1999, Johannessen et al., 2003). The data set consists of monthly mean values on $5^{\circ} \times 10^{\circ}$ latitude/longitude resolution and includes observations from Arctic land- and sea ice drifting station.

The spatial pattern of the wintertime (NDJFMA) warming is presented in the Fig. 2 as the anomaly (relative to the long-term mean, 1892-1998) of the SAT averaged over the period 1935-1944 (around the maximum warming time). As can be seen, the strongest warming (more than 2°C) occurred in the Kara- and Barents Seas and (to a smaller extent) in Baffin Bay. Significant warming (exceeding 1°C) covered the interior Arctic, eastern Siberia and northern part of the Greenland Sea. This pattern is rather robust, which is confirmed by the analysis of Arctic SAT trends (Johannessen et al., 2003) and EOF decomposition of the wintertime SAT variability in the Arctic (Semenov and Bengtsson, 2003). A very similar pattern was identified as the first EOF of the annual SAT variability in the Arctic (60°N - 85°N) for 1881-1980 (Kelly et al., 1981). The EOF decomposition of the SAT dataset (1892-1998) (not shown) also reveals a variability mode with maximum in the Kara and Barents Seas, which is found to be strongly related to the averaged Arctic temperature variability (Semenov and Bengtsson, 2003).

The pattern shown in the Fig. 2 is different to the temperature changes associated with large-scale atmospheric circulation variability patterns, such as, the NAO and SOI (Hurrell, 1996). At the same time, the regions of the largest warming are located in (or close to) the areas of the highest variability of the wintertime sea ice concentration (on interannual to interdecadal time scale) in the Barents and Greenland Seas (Venegas and Mysak, 2000; Deser et al., 2000). Thus, it is reasonable to assume that the warming pattern in the Barents-Greenland Seas reflects SAT variability associated with the wintertime sea ice changes.

A strong link between Arctic SAT and sea ice cover is evident from their opposite sign variations, which occur on different time scales including sea ice retreat in 1920s and 1930s (Zakharov, 1997). The sea ice data prior to the 1950s mostly consist of sporadic summer time observations. More reliable data are available from 1953 onwards (Walsh and Johnson, 1977; Chapman and Walsh, 1993), but only from 1978 are the data based on continuous satellite observations (Björge et al., 1997, Johannessen et al., 1999, Johannessen et al., 2003). Correlations between Arctic sea ice area, and SAT and sensitivity of the SAT to ice area changes ($|T/S_{ice}$) are shown in Table 1, in particular using Chapman and Walsh (1993) and Zakharov (1997) data (the Table 1 also shows correlations and sensitivities of the model calculations, which will be discussed in the Sections 3 and 4).

Table 1: Correlation between Arctic SAT and sea ice area (timeseries are detrended) and sensitivity ($|T/S_{ice}$) of Arctic SAT to sea ice change, °C/1 Mkm². Annual mean and wintertime (NDJFMA) data are used.

Observations	Correlation		$ T/S_{ice}$, °C/1 Mkm ²	
	Annual	Wintertime	Annual	Wintertime
Chapman and Walsh (1993), 1953-1998	-0.60	-0.52	-0.98	-1.43
Zakharov (1997), 1900-1993	-0.55		-1.44	
Model results				
ECHAM4/GISST*			-0.67	-1.13
ECHAM4/GISST 1951-1994 (ensemble mean)	-0.48	-0.62	-0.37	-0.68
ECHAM4/OPYC3 (200 yrs)	-0.68	-0.61	-1.40	-1.69

* these sensitivities are based on the ensemble mean changes [1955-1983]-[1910-1939]

3. Atmospheric modelling experiments

In order to analyze the sensitivity of the Arctic SAT to sea ice changes, we used ensemble simulations with the atmospheric model ECHAM4 (Roeckner et al., 1996). The model has 19 vertical levels and spatial resolution of approximately 2.8 deg in latitude and longitude. In the

numerical experiments, prescribed sea surface temperature (SST) and sea ice extent were used as boundary conditions. Observed changes in the greenhouse gases concentrations were included. An ensemble of four global simulations using the GISST2.2 SST/sea ice extent analysis for 1903-1994 (Rayner et al., 1996) as boundary conditions was carried out. The experiments started from slightly different initial atmospheric states, but all had identical surface boundary conditions. The large scale Northern Hemisphere circulation varied considerably between the four experiments. There is a discontinuity in the GISST2.2 sea ice data in 1949 (prior to 1949 only climatological sea ice data were used) due to introduction of a new procedure for sea ice concentration derivation (Rayner et al., 1996). This resulted in a sudden sea ice decrease of some 2 Mkm², Fig 3a. This is of course incorrect, but has here been used as a suitable boundary conditions for a sensitivity study as we found that the spatial distribution of ice extent changes and their typical seasonal variations features before and after 1949 were in general similar to the observed change 1978-1999 (Parkinson et al., 1999), in particular with the largest changes in the Barents Sea.

Time series of the wintertime (NDJFMA) Arctic SAT for ensemble mean and individual ensemble members and the corresponding sea ice area are shown in the Fig. 3a. Two 30-year periods have been chosen for the comparison representing high sea ice area values (1910-1939) and low ones (1954-1983). Corresponding sea ice extent changes and simulated (ensemble mean) SAT response are shown in Fig. 3b and c respectively. The results of the GISST simulations clearly show a strong response of the Arctic SAT to the imposed sea ice retreat in 1949 and following variability. The artificial 1949 sea ice decrease of 1.8 M.km² resulted in about 2.0 °C wintertime warming, Fig. 3a. As can be seen from the ensemble members' results, the area-averaged SAT increase is obviously exceeding the differences between the members of the ensemble. The warming is generally confined to the Arctic with largest changes (>6C) in the Barents Sea (Fig. 3b). SAT changes north of 60°N are statistically significant (exceeding two standard intra-ensemble deviations). The warming pattern in general follows the ice extent changes including strong warming in the Greenland Sea similar to the observed warming pattern (Fig. 2). The summer-half (MJJASO) SAT changes were much lower (0.9 °C and 2.3 M.km² respectively) and exhibited even some SAT decrease around the Pole in June. A similar negative trend to the north of 80°N in June was also found in the observational data during the 1920-1940 period (the warming phase). An overall comparison of the observed warming pattern and simulated SAT changes (Fig. 2

and 3b) reveals a close similarity. This suggests corresponding sea ice changes as a reason for the observed temperature variability. A quasi-stationary sensitivity of the Arctic temperature change to the sea ice (difference between two 30-year mean climates) results in -0.67 (-1.13) $^{\circ}\text{C}/\text{M km}^2$ for annual (wintertime) means. This is similar to the observed sensitivity (Table 1). The model sensitivity for the 1951-1994 period is lower due to ensemble averaging.

The simulated temperature increase in the areas of reduced ice extent is related to stronger oceanic heat flux to the atmosphere. This is illustrated in Fig. 4a and b, where the ice extent and surface turbulent heat loss (latent and sensible for the ensemble mean) changes (1954-1983 minus 1910-1939) are presented (DJF-values). The increased heat flux, exceeded $150\text{W}/\text{m}^2$ in the areas of the strongest ice extent decrease and about $20\text{W}/\text{m}^2$ for the Barents Sea average (corresponding to 40% sea ice decrease), generated an atmospheric circulation response. Sea level pressure (SLP) and wind anomalies (ensemble means) are shown in Fig. 4c and d, respectively. One can clearly see a cyclonic vortex and a negative pressure anomaly in the northeastern part of the Barents Sea associated with the surface heat source to the west to the Novaya Zemlya. The wind speed anomalies imply an advection of a relatively warm air from the southern Barents Sea to the Kara Sea and may also result in an increased wind-driven oceanic inflow through a western opening of the Barents Sea (not shown). This suggests a potential positive feedback mechanism, to be discussed in section 5.

4. Coupled atmosphere-ocean experiments

The model experiments described in section 3 only involved the atmospheric component of the climate system. In order to evaluate the role of ocean-sea ice-atmosphere feedbacks, and to search for a similar warming mechanism, we analyzed a control 300 year simulation with a coupled climate model ECHAM4/OPYC3 (Roeckner et al., 1999). The coupled model uses the same atmospheric model as was used in the sensitivity experiments described in the previous section. The concentrations of the greenhouse gases were set to the observed 1990 values. The model was run for 300 years with flux adjustment. Arctic sea ice area drifts for the first hundred years of the experiment, and so the analysis is restricted to the last 200 years of the simulation.

The model reproduces rather well the mean (9.8M km^2) and inter-annual variability (0.22M km^2) of Arctic sea ice area. The regions of the highest wintertime sea ice variations are located along the sea ice boundary in the Atlantic sector of the Arctic, with maximum variability in the Barents Sea. The model simulates warming events in high latitudes that resemble the observed early century warming, having comparable amplitude and spatial distribution, although of a shorter duration (Johannessen et al., 2003). The simulated Arctic SAT (60°N - 90°N) variability and sea ice area values (annual means) are shown in Fig.5a. The correlation between these timeseries is -0.77 (5-year running mean) or -0.70 (annual mean) and the sensitivity of the annual SAT to the sea ice changes is about $-1.4^\circ\text{C/M.km}^2$ (see Table 1). As can be seen from the correlations between annual mean Arctic sea ice and SAT (Fig.5b), the strongest temperature changes associated with sea ice cover variability are located in the Greenland-Barents-Kara Seas with a maximum in the Barents Sea. This pattern is rather similar to the observed warming pattern (Fig.2) and the SAT changes simulated by the atmospheric model (Fig.3b).

The sea ice cover variability in the Arctic is mainly determined by atmospheric conditions, through driving ocean currents that carry relatively warm and saline waters into the Arctic, and through wind-driven sea ice circulation. Particularly sensitive to the advective heat flux is the shallow (about 250 m) Barents Sea, where the highest variability of the wintertime sea ice coverage is found (both observed and simulated). An analysis of the coupled model results shows that the variation of the Barents Sea ice cover is determined by the oceanic volume inflow from the west. This is demonstrated by Figure 6, which shows simulated annual mean volume inflow to the Barents Sea, VIB, (in the upper 125 meters) through the Spitsbergen-Norwegian cross-section (about 20°E) and Arctic sea ice area. The figure demonstrates the role of this inflow for the sea ice variability. The correlation is -0.77 for the timeseries presented in the figure (5-year running mean) and -0.65 (annual). Several studies based on observational data (Dickson et al., 2000; Furevik, 2001) and model results (Loeng et al., 1997) have demonstrated that the VIB variation is linked to the wintertime atmospheric circulation. As was found in the coupled model simulation, the changes of the VIB are related to the corresponding variability of the SLP gradient over the western Barents Sea opening. This gradient, represented by the SLP difference between Spitsbergen and northernmost Norwegian coast, is proportional to the strength of geostrophical winds, which drive the surface current. The VIB and SLP gradient are shown in the Fig.7. The correlation is 0.42 (5-

years running mean) and 0.36 (annual data). Several periods can be seen, where decadal variations of the inflow and SLP gradient are particularly well related. A regression pattern of the SLP anomalies associated with VIB (not shown) shows a SLP dipole with maximum in northwestern Russia-Scandinavia and minimum stretched in the Greenland Sea. Some resemblance can be found between this pattern and one of the major atmospheric variability patterns in the high latitudes, the Barents Oscillation (Skeie, 2000).

5. Mechanism of the early century warming

A characteristic feature of the high latitude winter circulation in the 1930 and 1940s was the strong southwesterly to westerly flow through the passage between Spitsbergen and northern Norway. As can be seen from Fig 8 the strength of this flow, as deduced from the SLP difference, increased gradually during the 1920s by 6 ms^{-1} averaged for the winter season. As can further be seen, the Arctic surface temperature is highly related to the intensity of the geostrophic flow essentially for the whole century except of individual years of extreme flows. This suggests that it is the multi-year strength of the atmospheric flow into the Barents Sea region that controls the temperature of the Arctic. It is interesting to note that the NAO in the period 1920-1950 is uncorrelated to the Arctic temperature changes. This is not surprising since the NAO, as generally defined, represents the average strength of the eastern Atlantic westerly flow in the region between 65°N - 40°N .

Observations as well as modelling results show that the Barents Sea region has by far the largest inter-annual surface temperature variance and is the region that gives a major contribution to the temperature variations of the Arctic as a whole, Fig 2. It is also a region that is directly influenced by the net atmosphere and ocean heat transport into the Arctic. Observational studies (Dickson et al., 2000) show a clear relation between the wind driven volume flux and the temperature in the Barents Sea. Atmospheric experiments, discussed in section 3, show a distinct sensitivity of surface temperature to the extension of sea ice. We therefore hypothesize that the main cause of the Arctic warming was the increase of ocean heat transport into the Barents Sea, leading to reduced sea ice coverage and increased surface temperatures. It is reassuring to find from recently published data (Zakharov, 1997), discussed

in Johannessen et al. 2003, that during the 20th century early warming episode there was actually less sea ice in the Arctic than previously estimated (Chapman and Walsh, 1993).

As a possible feedback mechanism we suggest the associated increase in latent and sensible heat flux from the larger areas of open water in the Barents Sea. Surface heat fluxes during the cold season in the Barents Sea are large (the area is a pronounced winter heat source), with substantial inter-annual variations. Such an enhanced heat source will generate a vorticity source in the lower troposphere with lower surface pressure associated with the vorticity maximum. The circulation changes will maintain the southwesterly flow into the Barents Sea, and thus create a positive feedback (Fig 4). The correlation pattern between observed sea level pressure (Trenberth and Paolino, 1981) and Arctic surface temperature for the period 1920-1970 (Fig. 9) is consistent with this hypothesis. The result is underpinned by four atmospheric model experiments described in section 2. The sea ice data, GISST 2.2 (Rayner et al., 1996), were later found to be discontinuous, since the data set only included climatological sea ice data for the period before 1950. However, as has been shown, they were found useful to demonstrate the strong sensitivity of the Arctic temperature to sea ice variation. In all four experiments, a corresponding feedback mechanisms is suggested with lower surface pressure and enhanced positive vorticity in the experiments with reduced sea ice. It is further interesting to note that the mechanism is robust since all four experiments are very similar in this respect.

6. Conclusions

The Arctic 1920-1940 warming is one of the most puzzling climate anomalies of the 20th century. Over a period of some fifteen years the Arctic warmed by 1.7 °C and remained warm for more than a decade. This is a warming in the region comparable in magnitude what is to be expected as a consequence of anthropogenic climate change in the next several decades. A gradual cooling commenced in the late 1940s bringing the temperature back to much lower values although not as cold as before the warming started. Here, we have shown that this warming was associated and presumably initiated by a major increase in the westerly to south-westerly wind north of Norway leading to enhanced atmospheric and ocean heat transport from the comparatively warm North Atlantic Current through the passage between

northern Norway and Spitsbergen into the Barents Sea. It should be stressed that the increased winds were not related to the NAO, which in fact weakened during the 1920s and remained weak for the whole period of the warm Arctic anomaly. We have shown that the process behind the warming was most likely reduced sea ice cover, mainly in the Barents Sea. This is not an unexpected finding because of the climate effect of sea ice compared to that of an open sea, but intriguing since previously available sea ice data (Chapman and Walsh, 1993) did not indicate a reduced sea ice cover in the 1930s and 1940s. However, as we have shown here recent sea ice data sets (Johannessen et al., 2003 for a detailed presentation) actually showed a retreat in this period. Experiments with an atmospheric model forced with different sea ice data sets as well examination of a coupled model integration are in quantitative agreement with the observational data, broadly suggesting a 1°C warming for a reduction of the Arctic sea ice with 1 Mkm².

An evaluation of the coupled model suggests that a major part of the warming is caused by transport of warm ocean water, in the upper most 125 m of the ocean model, into the Barents Sea, driven by stronger than the normal surface winds.

The question as to the cause of the enhanced westerly winds is an open question and we can here only offer possible explanations. Contrary to other studies (Stott et al., 2000), we suggests that the warm Arctic event just happened by chance through an aggregation of several consecutive winters with pronounced high latitude westerly in the Atlantic sector. High latitude warm events are possible as has been demonstrated by Delworth and Knutsson, (2000) and Johannessen et al., (2003) and are being generated during the course of a long integration with a coupled model. However, an important factor in setting up a long lasting event is the indication, both in observations and in the modeling studies, of a dynamical feedback mechanism related to the generation of an atmospheric heat source in the Barents Sea and an associated creation of a cyclonic circulation. Such a circulation will, as we have demonstrated, act to maintain the westerly to southwesterly atmospheric flow into the region and the associated heat transport. Alternatively, if sea ice has become more extensive in the Barents Sea any tendency to westerly inflow would be weakened acting to prolong the conditions for an extensive sea ice cover.

Needless to say, a necessary condition for the Arctic warming event to commence depends on changes in the large scale atmospheric circulation. A comprehensive discussion of this is outside the scope of this study. As discussed in the introduction, there are many possibilities. Our view is that natural processes in the climate system are the most likely cause, at least there are hardly any information neither from observations nor from model experiments to the opposite. In fact we have reasons to believe that the natural variability of the ECHAM 4/OPYC model rather is underestimated. The latest MPI coupled model experiment (without flux correction) (M.Latif pers. communication) has stronger multi-decadal anomalies. We further believe that anthropogenic effects are unlikely because of the modest forcing in the early part of the last century and if it would be the case the climate feedback would be much stronger than estimated and inconsistent with present observations. Solar forcing cannot be excluded as a possible hypothesis (Lean and Rind, 1998) but suffers from the uncomfortable fact that it is not supported by direct observations.

Observational data in the Arctic from the first part of the 20th century are relatively sparse in particular from the Arctic Ocean. The gridded data sets of surface temperature and sea ice are essentially constructed from a limited number of observations, although the auto-correlation structure used in the analyses are calculated from present data. However, observations from the most sensitive region, Barents Sea are fairly good and better than previously thought, which means that we can have reasonable confidence in the result.

What consequences may the findings of this study have for the possible evolution of the Arctic climate? Notwithstanding an expected overall climate warming it is suggested that the Arctic climate would be exposed to considerable internal variations over several years initiated by stochastic variations of the high latitude atmospheric circulation and subsequently enhanced and maintained by sea ice feedback. The Barents Sea region is identified as particular sensitive area in this respect. Realistic simulation of the Arctic climate consequently requires an accurate representation of atmosphere-ocean-sea ice feedback processes.

Acknowledgements

We are thankful to Noel Keenlyside for many useful comments on the text. This study was supported by funding from the European Union within the Arctic Ice Cover Simulation Experiment project (contract No. EVK2-CT-2000-00078 AICSEX).

References

Alekseev, G. V., Alexandrov, Ye., I., Bekriayev, R. V., Svyashchennikov, P. N., and N. Ye. Harlanienkova, 1999: Detection and modelling of greenhouse warming in the Arctic and sub-Arctic. INTAS 97 – 1277, Technical Report on Task 1: Surface air temperature from meteorological data. Arctic and Antarctic Research Institute, St. Petersburg, Russia.

Andronova, N. G., and M. E. Schlesinger, 2000: Causes of global temperature changes during the 19th and 20th centuries. *Geophys. Res. Lett.*, **27**, 2137-2140.

Beer, J., Mende, W., and R. Stellmacher, 2000: The role of the sun in climate forcing. *Quaternary Science Review*, **19**, 403-415.

Bengtsson, L., 2001: Uncertainties of global climate prediction. In: Global Biogeochemical Cycles in the Climate System. Eds. E.-D. Schulze, M. Heimann, S. Harrison, E. Holland, J. Lloyd, I. C. Prentice, D. Schimel. Academic Press, New York, p. 15-29.

Bengtsson, L., Roeckner, E., and M. Stendel, 1999: Why is the global warming proceeding much slower than expected? *J. Geophys. Res.*, **104**, 3865-3876.

Björge, E., O. M. Johannessen, and M. W. Miles, 1997: Analysis of merged SMMR-SSMI time-series of Arctic and Antarctic sea ice parameters 1978-1995. *Geophys. Res. Lett.*, **24**, 413-416.

Callendar, G. S., 1938: The artificial production of carbon dioxide and its influence on temperatures. *Quart. J. Roy. Meteor. Soc.*, **64**, 223-227.

Chapman, W. L., and J. E. Walsh, 1993: Recent variations of sea ice and air temperature in high latitudes. *Bull. Amer. Meteorol. Soc.*, **74**, 33-47.

Cubasch, U., Voss, R., Hegerl, G. C., Waszkewitz, J., and T. J. Crowley, 1997: Simulation of the influence of solar radiation variations on the global climate with an ocean-atmosphere general circulation model. *Climate Dyn.*, **13**, 757-767.

Cubasch, U., and R. Voss, 2000: The influence of total solar irradiance on climate. *Space Science Rev.*, **94**, 185-198.

Curry, R. D., and M. S. McCartney, 2001: Ocean gyre circulation changes associated with the North Atlantic Oscillation. *J. Phys. Oceanogr.*, **31**, 3374-3400.

Delworth, T. L., and T. R. Knutson, 2000: Simulation of early 20th century global warming. *Science*, **287**, 2246-2250.

Delworth, T.L., and M.E. Mann, 2000: Observed and simulated multidecadal variability in the Northern Hemisphere, *Climate Dyn.*, **16**, 661-676.

Deser, C., Walsh, J. E., and M. S. Timlin, 2000: Arctic sea ice variability in the context of recent atmospheric circulation trends. *J. Climate*, **13**, 617-633.

Dickson, R.R., Osborn, T.J., Hurrell, J.W., Meincke, J., Blindheim, J., Adlandsvik, B., Vinje, T., Alekseev, G., and W. Maslowski, 2000: The Arctic Ocean response to the North Atlantic oscillation. *J. Climate*, **13**, 2671-2696.

Friis-Christensen, E., and K. Lassen, 1991: Length of the solar cycle – an indicator of solar activity closely associated with climate. *Science*, **254**, 698-700.

Fröhlich, C., and J. Lean, 1998: The Sun's total irradiance: Cycles, trends and related climate change uncertainties since 1976. *Geophys. Res. Lett.*, **25**, 4377-4380.

Furevik, T., 2001: Annual and interannual variability of Atlantic Water temperatures in the Norwegian and Barents Seas: 1980-1996. *Deep-Sea Research I*, **48**, 383-404.

Hansen, J., Sato, M., and R. Ruedy, 1997: Radiative forcing and climate response. *J. Geophys. Res.*, **102**, 6831-6864.

Hansen, J., Ruedy R., Glascoe J., and M. Sato, 1999: GISS analysis of surface temperature change. *J. Geophys. Res.*, **104**, D24, 30997-31022.

Hasselmann, K., 1997: Multi-pattern fingerprint method for detection and attribution of climate change. *Climate Dyn.*, **13**, 601-611.

Hegerl., G. S., Hasselmann, K., Cubasch, U., Mitchell, J. F. B., Roeckner, E., Voss, R., and J. Waszkewitz, 1997: Multi-fingerprint detection and attribution analysis of greenhouse gas, greenhouse gas-plus-aerosol and solar forced climate change. *Climate Dyn.*, **13**, 613-634.

Hoerling, M. P., Hurrell, J. W., and T. Y. Xu, 2001: Tropical origins for recent North Atlantic climate change. *Science*, **292**, 90-92.

Hoyt, D. V., and K. H. Schatten, 1993: A discussion of plausible solar irradiance variations, 1700-1992. *J. Geophys. Res.*, **98**, 18895-18906.

Hurrell, J. W., 1995: Decadal trends in the North Atlantic Oscillation. Regional temperature and precipitation. *Science*, **269**, 676-679.

Hurrell, J. W., 1996: Influence of variations in extratropical wintertime teleconnections on Northern Hemisphere temperature. *Geophys. Res. Lett.*, **23**, 665-668.

Johannessen, O. M., Shalina, E. V., and M. W. Miles, 1999: Satellite evidence for an Arctic sea ice cover in transformation. *Science*, **286**, 1937-1939.

Johannessen, O. M., Bengtsson, L., Kuzmina, S. I., Miles, M. W., Semenov, V. A., Hasselmann, K., Cattle, H. P., Alekseev, G. V., Nagurny, A. P., Zakharov, V. F., Bobylev, L. P., and L. H. Pettersson: Arctic climate change – Will the ice disappear this century? Submitted to *Tellus*.

Johnson, M.A., Proshutinsky, A.Y., and I.V. Polyakov, 1999: Atmospheric patterns forcing two regimes of arctic circulation: A return to anticyclonic conditions? *Geophys. Res. Lett.*, **26**, 1621-1624.

Jones, P. D., New, M., Parker, D. E., Martin, S., and I. G. Rigor, 1999: Surface air temperature and its changes over the past 150 years. *Reviews Geophys.*, **37**, 173-199.

Joos, F., and M. Bruno, 1998: Long-term variability of the terrestrial and oceanic carbon sinks and the budgets of the carbon isotopes ¹³C and ¹⁴C. *Glob. Biogeochem. Cycles*, **12**, 277-295.

Kahl, J. D., Charlevoix, D. J., Zaitseva, N. A., Schnell, R. C., and M. C. Serreze, 1993: Absence of evidence for greenhouse warming over the Arctic Ocean in the past 40 years. *Nature*, **361**, 335-337.

- Kelly, P. M., Jones, P. D., Sear C. B., Cherry, B. S. G., and R. K. Tavakol, 1982: Variations in surface air temperatures: Part 2. Arctic regions, 1881-1980. *Mon. Wea. Rev.*, **110**, 71-83.
- Lean, J., and D. Rind, 1998: Climate forcing by changing solar radiation. *J. Climate*, **11**, 3069-3094.
- Loeng, H., Ozhigin, V., and B. Adlandsvik, 1997: Water fluxes through the Barents Sea. *ICES J. Marine Science*, **54**, 310-317.
- Mysak, L.A., and S.A. Venegas, 1998: Decadal climate oscillations in the Arctic: A new feedback loop for atmosphere-ice-ocean interactions. *Geophys. Res. Lett.*, **25**, 3607-3610.
- Mysak, L.A., 2001: Patterns of Arctic circulation. *Science*, 293, 1269-1270.
- Martin, S., Munoz, E. A., and R. Drucker, 1997: Recent observations of a spring-summer surface warming over the Arctic Ocean. *Geophys. Res. Lett.*, **24**, 1259-1262.
- Parkinson, C. L., Cavalieri, D. J., Gloersen, P., Zwally, H.J., and J. C. Comiso, 1999: Arctic sea ice extents, areas, and trends, 1978-1996. *J. Geophys. Res.*, **104**, 20 837-20 856.
- Polyakov, I. V., and M. A. Johnson, 2000: Arctic decadal and interdecadal variability. *Geophys. Res. Lett.*, **27**, 4097-4100.
- Polyakov, I. V., Alekseev, G. V., Bekryaev, R. V., Bhatt, U., Colony, R. L., Johnson, M. A., Karklin, V. P., Makshtas, A. P., Walsh, D., and V. Yulin, 2002: Observationally based assessment of polar amplification of global warming. *Geophys. Res. Lett.*, **29**, 1878.
- Przybylak, R., 2000: Temporal and spatial variations of surface air temperature over the period of instrumental observations in the Arctic. *Int. J. Climatology*, **20**, 587-614.
- Räisänen J., 2002: CO₂-induced changes in interannual temperature and precipitation variability in 19 CMIP2 experiments. *J. Climate*, **15**, 2395-2411.
- Rayner, N. A., Harten, E. B., Parker, D. E., Folland, C. K., and R. B. Hacked, 1996: Version 2.2 of the global sea-ice and sea surface temperature data set, 1903-1994. Clim. Res. Tech. Note CRTN74, Bracknell, UK, 1996.
- Reid, G. C., 1991: Solar total irradiance variations and the global sea-surface temperature record. *J. Geophys. Res.*, **96**, 2835-2844.

Rigor, I. G., Colony, R. L., and S. Martin, 2000: Variations in surface air temperature observations in the Arctic, 1979-97. *J. Climate*, **13**, 896-914.

Robock, A., 2000: Volcanic eruptions and climate. *Reviews Geophys.*, **38**, 191-219.

Roeckner, E., Arpe, K., Bengtsson, L., Christoph, M., Claussen, M., Dümenil, L., Esch, M., Giorgetta, M., Schlese, U., and U. Schulzweida, 1996: The atmospheric general circulation model ECHAM-4: Model description and simulation of present-day climate. Max Planck Institute for Meteorology Rep. 218, Hamburg, Germany, 90 pp.

Roeckner, E., Bengtsson, L., Feichter, J., Lelieveld, J., and H. Rodhe, 1999: Transient climate change simulations with a coupled atmosphere-ocean GCM including the tropospheric sulfur cycle. *J. Climate*, **12**, 3004-3032.

Schlesinger, M. E., and N. Ramankutty, 1994: An oscillation in the global climate system of period 65-60 years. *Nature*, **367**, 723-726.

Schneider, E. K., Bengtsson, L., and Z.-Z. Hu, 2003: Forcing of northern hemispheric climate trends. *J. Atmos. Sci.* (in print).

Semenov, V., and L. Bengtsson, 2003: Modes of the wintertime Arctic temperature variability. Max Planck Institute for Meteorology Rep. 343, Hamburg, Germany, 18 pp.

Serreze, M. C., Walsh, J. E., Chapin III, F. S., Ostercamp, T., Dyurgerov, M., Romanovsky, V., Oechel, W. C., Morison, J., Zhang, T., and R. G. Barry, 2000: Observational evidence of recent change in the northern high-latitude environment. *Climatic Change*, **46**, 159-207.

Skeie, P., 2000: Meridional flow variability over Nordic seas in the Arctic Oscillation framework. *Geophys. Res. Lett.*, **27**, 2569-2572.

Stott, P. A., Tett, S. F. B., Jones, G. S., Allen, M. R., Mitchell, J. F. B., Jenkins, G. J., 2001: External control of 20th century temperature by natural and anthropogenic forcings. *Science*, **290**, 2133-2137.

Tett, S. F. B., Stott, P. A., Allen, M. R., Ingram, W. J., and J. F. B. Mitchell, 1999: Causes of twentieth-century temperature change near the Earth's surface. *Nature*, **399**, 569-572.

Trenberth, K. E., and D. A. Paolino, 1980: The Northern Hemisphere sea-level pressure data set – trends, errors and discontinuities. *Mon. Wea. Rev.*, **108**, 855-872.

Venegas, S. A., and L. A. Mysak, 2000: Is there a dominant time scale of natural variability in the Arctic? *J. Climate*, **13**, 3412-3434.

Walsh, J. E. and C. M. Johnson, 1979: An analysis of Arctic sea ice fluctuations, 1953-77. *J. Phys. Oceanogr.*, **9**, 580-591.

Wunsch, C., 1999: The interpretation of short climate records, with comments on the North Atlantic and Southern Oscillations. *Bull. Amer. Meteorol. Soc.*, **80**, 245-255.

Zakharov, V. F., 1997: *Sea ice in the climate system*. World Climate Research Programme/Arctic Climate System Study, WMO/TD-No.782, Geneva, 80 pp.

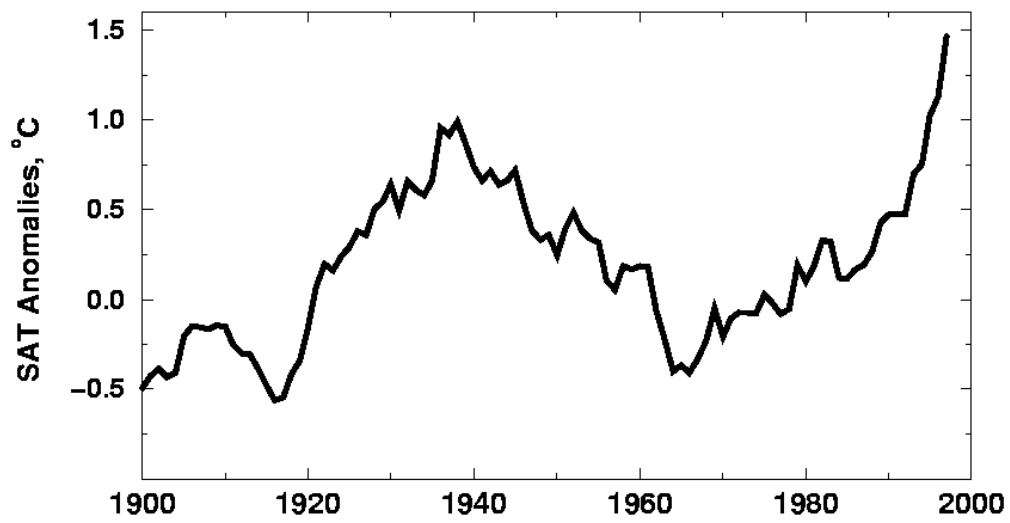


Figure 1: Annual mean Arctic SAT anomalies (in °C, area averaged from 60°N to 90°N) from Johannessen et al. (2003), 5-year running mean.

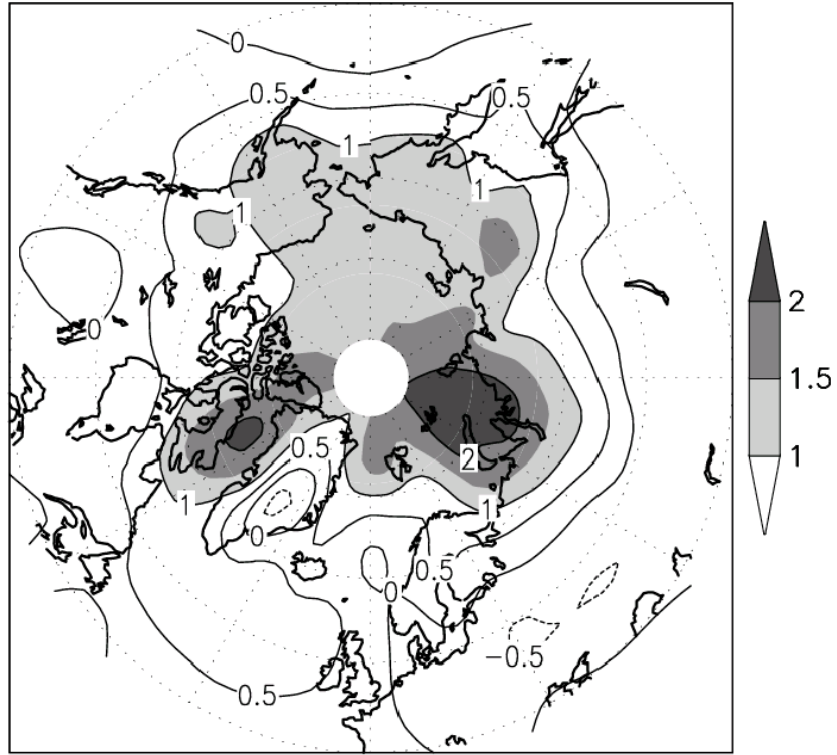


Figure 2: 1935-1944 wintertime (NDJFMA) Arctic SAT anomaly, in °C (relative to the long-term mean, 1892-1998).

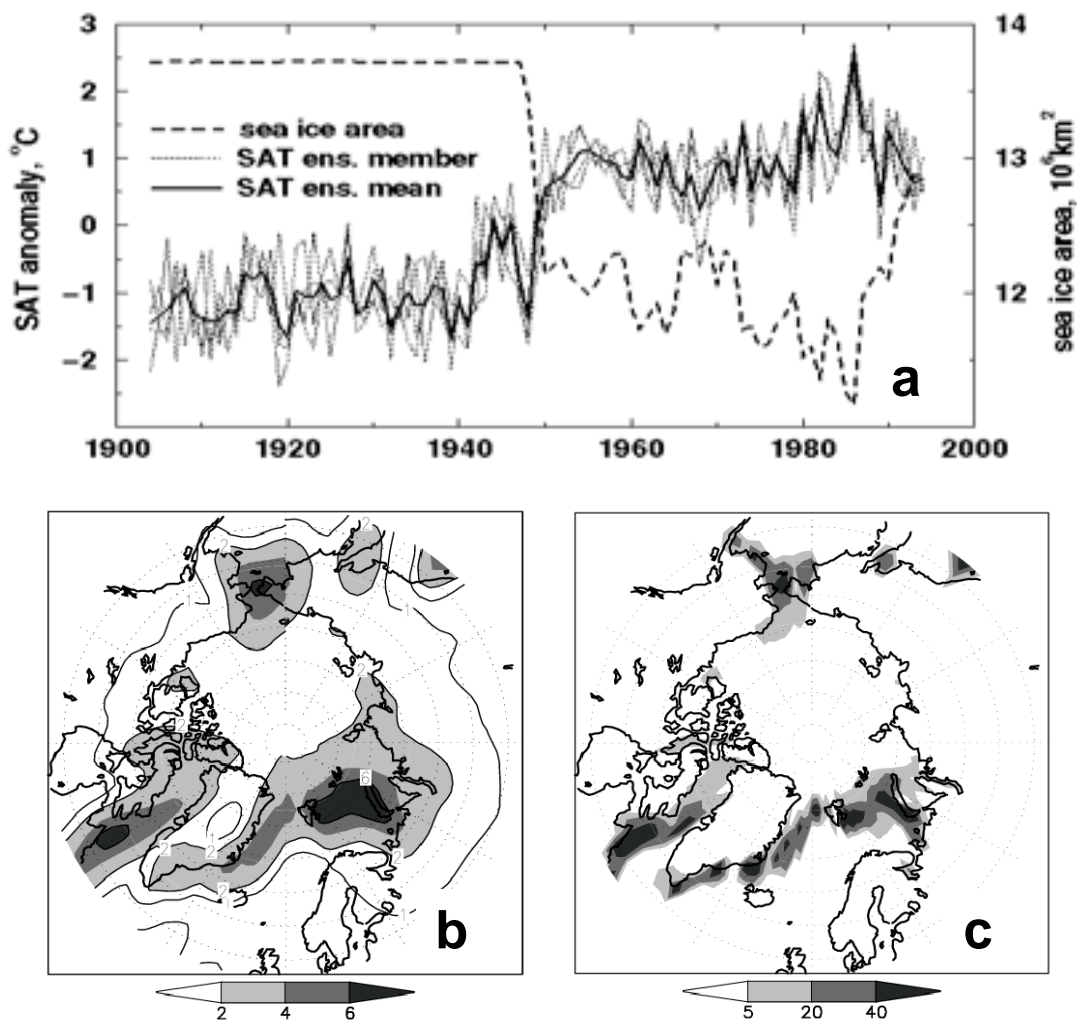


Figure 3: (a) Wintertime Arctic SAT anomalies (in °C) simulated by an ensemble of four experiments with the ECHAM4 model using prescribed SST/sea ice boundaries (GISST2.2). Ensemble mean (thick solid) and ensemble members (thin solid) are shown. Thick dashed line is Arctic sea ice area, M. km²; (b) wintertime SAT difference (in °C) (ECHAM4/GISST2.2.ensemble mean) between the 1954-1983 and 1910-1939 averages representing “low” and “high” sea ice conditions respectively; (c) wintertime sea ice concentration differences (in percent) between the 1910-1939 and 1954-1983 averages.

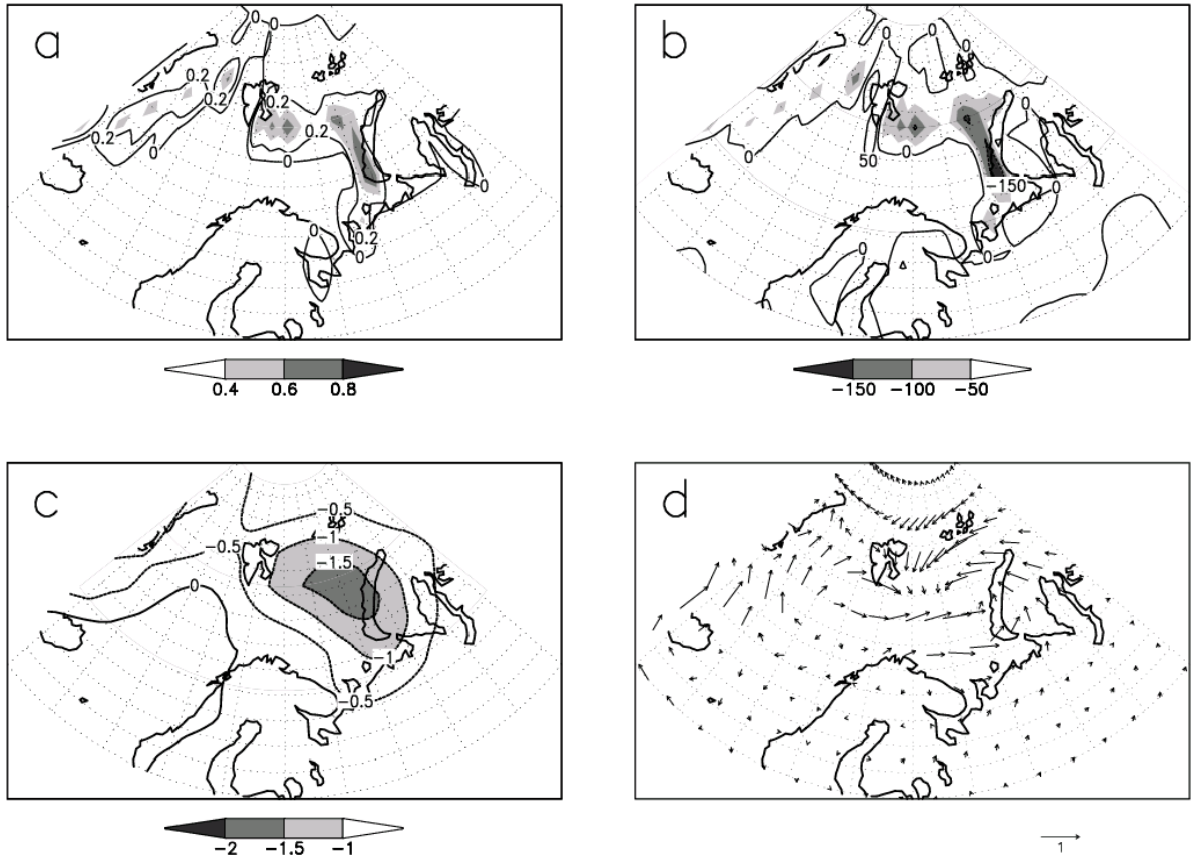


Figure 4: Simulated ensemble mean DJF difference (1954-1983)-(1910-1939) for (a) sea ice concentrations (fraction), (b) turbulent (latent and sensible) surface heat flux, Wm^2 , (c) sea level pressure, mb, and (d) 10m wind speed.

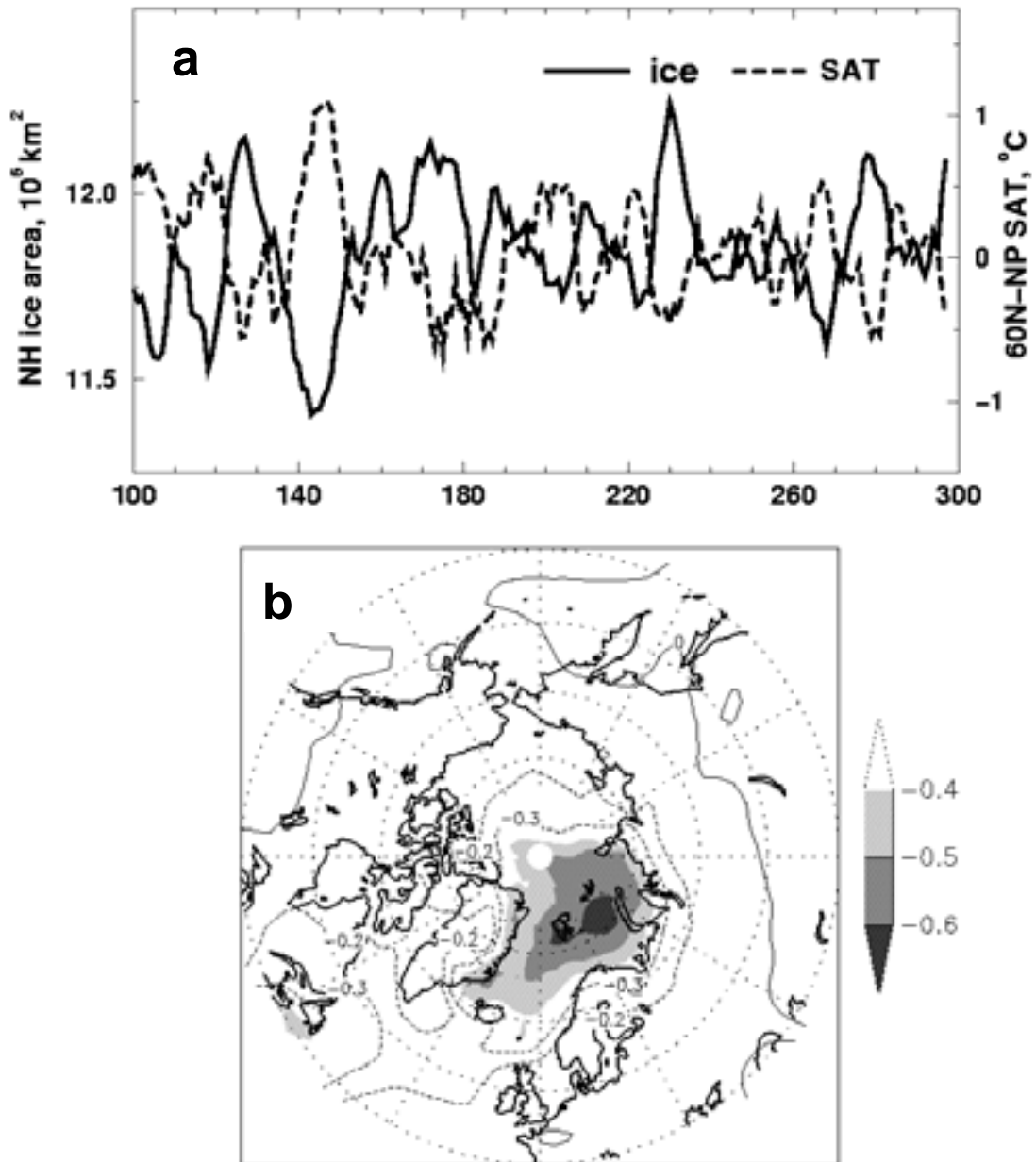


Figure 5: (a) Wintertime Arctic SAT anomalies (60°N to 90°N , in $^{\circ}\text{C}$) and sea ice area (M. km^2) as simulated by the ECHAM4/OPYC3 coupled GCM in a control experiment (5-year running mean), the correlation between the two curves is -0.76 ; (b) correlation between averaged wintertime Arctic sea ice coverage and local surface air temperatures.

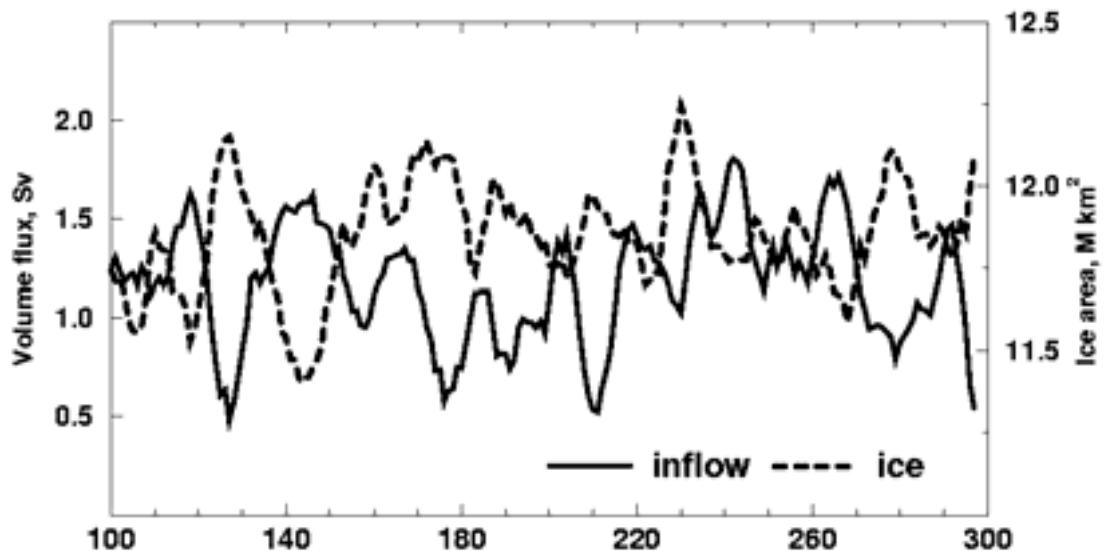


Figure 6: ECHAM4/OPYC3 control simulation: wintertime Arctic sea ice area (M. km^2) and oceanic volume inflow (upper 125 m) into the Barents Sea (Sv), 5-year running mean. The correlation between these timeseries is -0.77 .

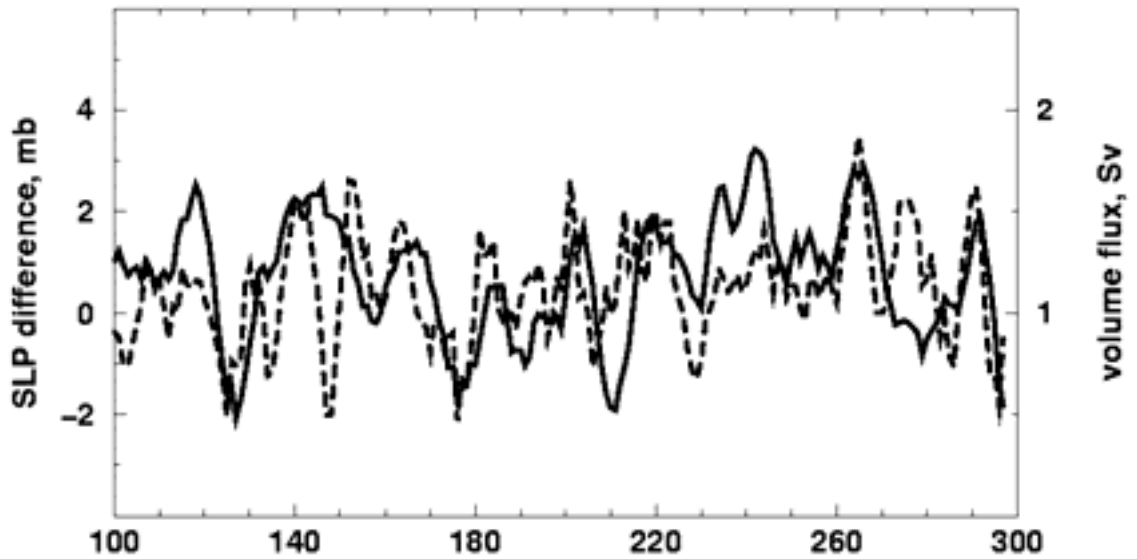


Figure 7: ECHAM4/OPYC3 control simulation: annual mean oceanic volume inflow (upper 125 m) into the Barents Sea (Sv, solid) and DJF SLP difference between Spitsbergen and the northernmost Norwegian coast (mb), 5-year running mean (dashed). The correlation between the timeseries is 0.42.

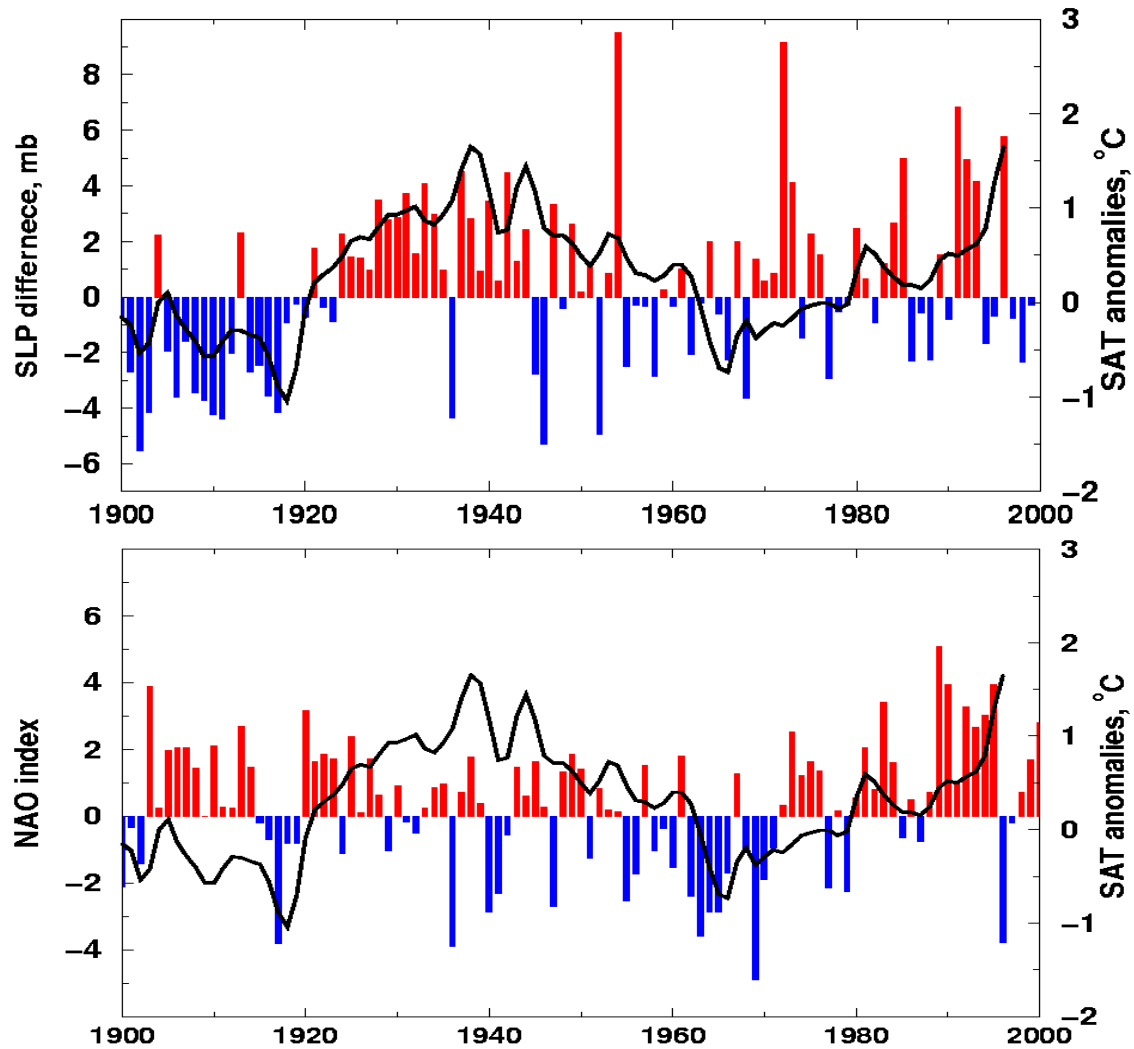


Figure 8: (a) DJF SLP difference between Spitsbergen and the northernmost Norwegian coast (mb, vertical bars) and annual mean Arctic SAT anomalies ($^{\circ}\text{C}$, 5-year running mean, solid line); (b) the NAO index and SAT anomalies as in (a).

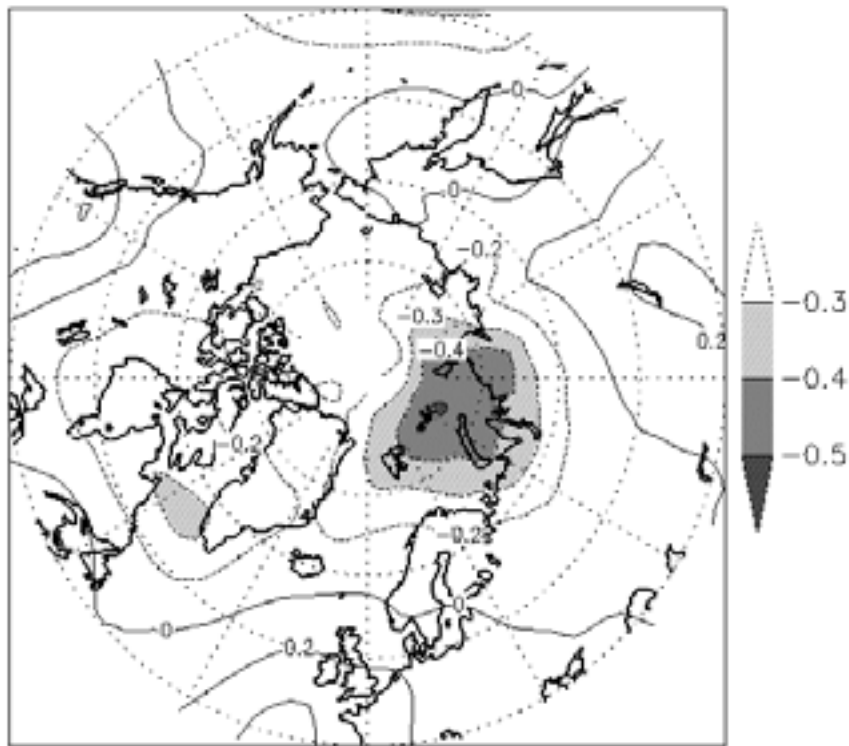


Figure 9: Correlation between Arctic (60°N - 90°N area averaged) wintertime SAT anomalies and DJF SLP for the 1920-1970 period.